Original Article
Yonsei Med J 2022 Jul;63(7):657-664
https://doi.org/10.3349/ymj.2022.63.7.657
Yonsei Medical Journal
YMJ
pISSN: 0513-5796 · eISSN: 1976-2437

Does the Suprascapular Nerve Move within the Suprascapular Notch? Biomechanical Perspective Using the Finite Element Method

Yon-Sik Yoo[1]*, Seong-wook Jang[2]*, Yoon Sang Kim[3], Jung-Ah Choi[4], Jung Hyun Oh[5], and Jeung Yeol Jeong[5]

[1]Camp 9 Orthopedic Clinic, Hwaseong;
[2]Assistive Technology Research Team for Independent Living, Research Institute, National Rehabilitation Center, Seoul;
[3]BioComputing Lab, School of Computer Science and Engineering, Korea University of Technology and Education, Cheonan;
Departments of [4]Radiology and [5]Orthopedic Surgery, Hallym University Dongtan Sacred Heart Hospital, Hallym University College of Medicine, Hwaseong, Korea.

Purpose: We aimed to analyze changes in suprascapular nerve (SSN) position within the suprascapular notch during in vivo shoulder abduction.

Materials and Methods: Three-dimensional models of the shoulder complex were constructed based on magnetic resonance imaging of the brachial plexus (BP-MR) in a patient diagnosed with SSN dysfunction but normal scapular movement. Using BP-MR in neutral position and computed tomography data on shoulder abduction, shoulder abduction was simulated as the transition between two positions of the shoulder complex with overlapping of a neutral and abducted scapula. SSN movement during abduction was evaluated using the finite element method. Contact stress on the SSN was measured in the presence and absence of the transverse scapular ligament (TSL).

Results: In the neutral position, the SSN ran almost parallel to the front of the TSL until entering the suprascapular notch and slightly contacted the anterior-inferior border of the TSL. As shoulder abduction progressed, contact stress decreased due to gradual loss of contact with the TSL. In the TSL-free scapula, there was no contact stress on the SSN in the neutral position. Towards the end of shoulder abduction, contact stress increased again as the SSN began to contact the base of the suprascapular notch in both TSL conditions.

Conclusion: We identified changes in the position of the SSN path within the suprascapular notch during shoulder abduction. The SSN starts in contact with the TSL and moves toward the base of the suprascapular notch with secondary contact. These findings may provide rationale for TSL release in SSN entrapment.

Key Words: Suprascapular nerve entrapment, transverse scapular ligament decompression, scapular movement, finite element analysis

Received: September 10, 2021 **Revised:** March 18, 2022
Accepted: March 29, 2022
Corresponding author: Jeung Yeol Jeong, MD, Department of Orthopedic Surgery, Hallym University Dongtan Sacred Heart Hospital, Hallym University College of Medicine, 7 Keunjaebong-gil, Hwaseong 18450, Korea.
Tel: 82-31-8086-2410, Fax: 82-31-8086-2029, E-mail: inzaghy@naver.com

*Yon-Sik Yoo and Seong-wook Jang contributed equally to this work.
•The authors have no potential conflicts of interest to disclose.

INTRODUCTION

Suprascapular nerve (SSN) entrapment syndrome occurs because the surrounding anatomy of the SSN renders it vulnerable to injury and compression.[1] In particular, a stenotic notch due to the presence of a thick transverse proximal ligament is considered a patho-anatomical risk factor because it can cause compression of the SSN proper or the motor branch to the supraspinatus muscle travelling through the suprascapular notch underneath the transverse scapular ligament (TSL).[2-6]

TSL release is considered a reasonable surgical option in pa-

tients with clinical symptoms of SSN entrapment who show irreversible changes in signal intensity within the supraspinatus and infraspinatus muscles on magnetic resonance (MR) imaging and decreased muscle contractibility or nerve conduction velocity.[7-10] However, since most chronic patients show positive findings on either MR or electromyography, the indication for TSL release is difficult in patients with relative short symptom duration without these positive findings.[11,12]

Clinically, SSN entrapment manifests as a radiologically proven stenotic suprascapular notch. However, from a biomechanical perspective, the SSN may undergo dynamic entrapment due to scapular movement.[13] Therefore, even if there is no evidence of nerve entrapment on radiological or electromyography studies with the scapula in a neutral position, the SSN may still be susceptible to entrapment during scapular movement if the notch is stenotic due to TSL ossification.[14] While the possibility of dynamic SSN entrapment is recognized, its patho-mechanics remain poorly understood because no biomechanical data on this topic have been reported in the literature.

In this study, we aimed to characterize the movement of the SSN within the suprascapular notch in vivo. For this purpose, we first constructed a complex three-dimensional (3D) model of the should complex, comprising the cervical spine, upper cervical root, and the brachial plexus (BP), including the SSN (BP-SSN), in a patient with SSN entrapment syndrome but normal scapular movement. We then recorded changes in SSN position within the suprascapular notch during simulated shoulder abduction. We also analyzed contact stress patterns on the SSN within the scapular notch during simulated shoulder abduction in the presence and absence of the TSL. We hypothesized that there would be a change in position of the SSN path within the scapular notch according to the shoulder movement and that contact stress in the TSL would increase.

MATERIALS AND METHODS

Study design

The study was approved by the Institutional Review Board at Hallym University College of Medicine, Dongtan Sacred Heart Hospital (No. 2018-02-003) and was conducted in agreement with the principles of the Declaration of Helsinki. Written informed consent was obtained from the patient included in this study. Primary institution where this investigation was performed: Hallym University Dongtan Sacred Heart Hospital.

We considered eight patients who underwent diagnostic MR and computed tomography (CT) for diagnostic purposes before being indicated for TSL release. Four patients had clinical signs and positive investigations substantiating SSN involvement, such as wasting of the supraspinatus and infraspinatus, as well as decreased muscle volume on MR or prolonged nerve conduction velocity stimulation. The remaining four patients had negative investigations despite strong clinical manifestation of SSN entrapment and hence underwent magnetic resonance imaging of the brachial plexus (BP-MR) and cervical spine, electromyography, and nerve conduction velocity studies to rule out proximal lesions. Dynamic entrapment of the SSN due to dynamic interaction between the SSN and TSL was suspected in these four patients with deep posterior shoulder pain and discomfort during range of movement assessment of shoulder. For the present study, we selected one patient who exhibited an identifiable TSL and scapular position symmetry on CT, as well as normal patterns of scapula movement.

We used preoperative data of BP-MR images in the neutral arm position and CT images in an arm abduction position to obtain 3D models of the shoulder complex and simulate shoulder abduction.

We analyzed SSN positional and contact stress data during simulated abduction of the TSL-bound and TSL-free scapula.

Construction of 3D models of the shoulder complex based on MR images

The models of the shoulder complex, which included bony structures (cervical spine, upper cervical root, and rib; part of the scapula) and nerve systems (BP-SSN, cervical spinal cord), were reconstructed from MR images obtained using a 3T scanner (Magnetom Skyra; Siemens, Erlangen, Germany) (Fig. 1A). To enable multi-plane reconstruction of the 3D models, we used T2-weighted axial, oblique sagittal, and coronal sequences with fat suppression according to the Dixon method,[15] as well as T1-weighted, coronal, fat-suppressed, volumetric interpolated breath-hold examination sequences.

Two authors, orthopedic surgeons, (J.Y.J and Y.S.Y) used a 0.7-mm paintbrush to manually segment the BP-SSN, spinal-rib complex, and part of the scapula on each slice obtained from sequences in different planes (axial, coronal, and sagittal). Part of the BP-SSN was reconstructed semi-automatically using a volume ray casting method[16] after removing noise and undesired objects (bones, heart, aortic arch, arteries, veins, and trachea). The undesired objects were removed sequentially through iterative volume ray casting with different threshold values. The SSN was segmented from the BP upper trunk to the site of branching at the spinoglenoid notch.

Once the BP was segmented for each plane, we combined the 3D BP reconstructions in order to assemble the entire course of the SSN. Using computer-aided design, the SSN was remodeled as a cylindrical tube with a diameter of 2 mm (Fig. 1B).[17] The SSN models migrated from C5 nerve to suprascapular notch to avoid a collision with the TSL, anterior scalene muscle, and middle scalene muscle. The TSL, which is usually not distinguishable on MR images, was reconstructed by referring to the identifiable bone remnants of the posterior coracoid process and the medial margin of the suprascapular notch on the CT image. According to a previous method,[18] we determined that the TSL had a width of 8 mm and a thickness of 2 mm, similar to the thickness of the scapular wall (Fig. 1C). Moreover, we

https://doi.org/10.3349/ymj.2022.63.7.657

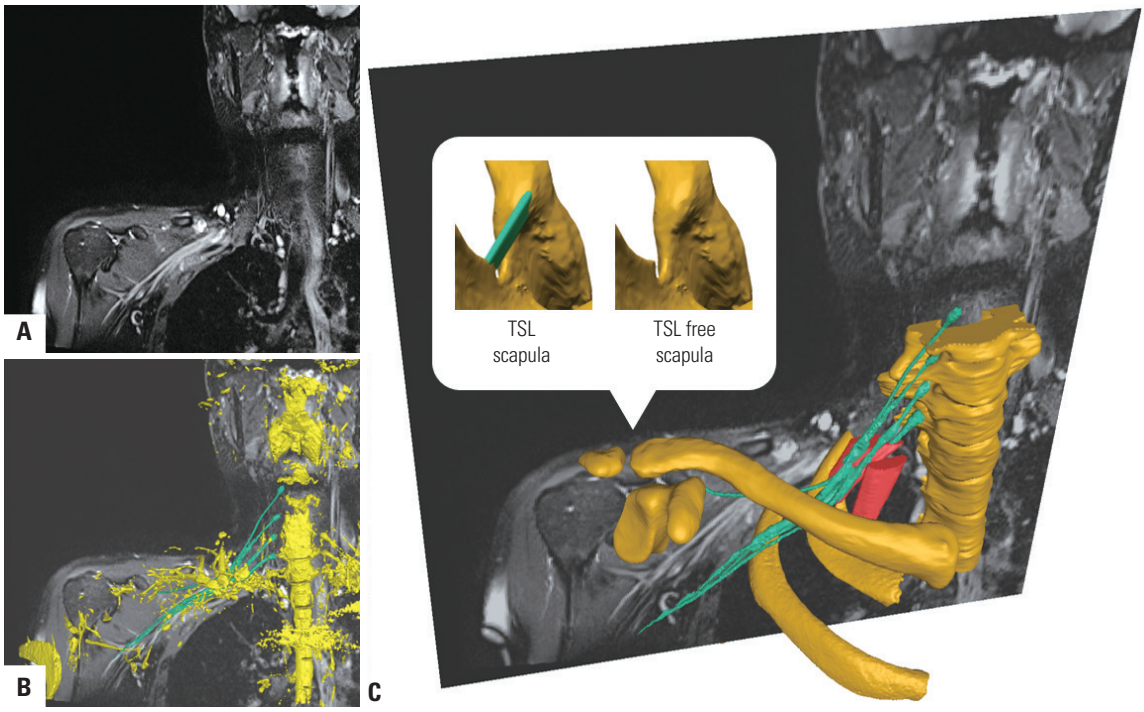

Fig. 1. Process of 3D model reconstruction from BP-MR images. (A) Representative BP-MR image that includes an identifiable BP, including the SSN and spine-rib-scapula complex. (B) Primitive 3D BP-SSN models obtained by means of isosurface extraction from BP-MR images. (C) 3D models of the shoulder containing the spine-rib complex, anterior scalene muscle, middle scalene muscle, clavicle, coracoid process, and TSL. The TSL model was recreated with reference to the identifiable bone remnants of the posterior coracoid process and lateral wall of the suprascapular notch on computed tomography. 3D, three-dimensional; BP-MR, magnetic resonance imaging of the brachial plexus; SSN, suprascapular nerve; TSL, transverse scapular ligament.

included the clavicle, thoracic rib bones, and anterior and posterior edges of the scalene muscles because we believe that these structures affect the motion of the SSN.

Simulating shoulder abduction

In order to simulate shoulder abduction in vivo, we used preoperative CT images together with the BP-MR images. The CT (SOMATOM Definition FLASH; Siemens) (peak kilovoltage, 120; bone algorithm reconstruction; slice thickness, 0.7 mm) images in the coronal, axial, and sagittal planes were obtained with the patient in the supine position, with 90° arm abduction.[19] To ensure that the same shoulder abduction angle was obtained bilaterally, the patient held their palms in supination with both arms abducted 90° and with the elbows flexed, keeping the palms touching the forehead. The CT scan was taken from the upper cervical spine to the lower part of the scapula.

We simulated in vivo 3D movement from the neutral to the abducted position of the scapula. The movement involved upward rotation, posterior tilt, and external rotation in a standard joint coordinate system defined in accordance with the recommendations of the International Society of Biomechanics.[20] The neutral and abducted scapula were defined based on the superimposition of the spine-rib complex in the neutral (MR images) and abducted (CT images) positions. To minimize errors, we defined the neutral position in terms of the upper cervical and thoracic spine together with the first and second ribs, which are less affected by respiration and posture (Fig. 2A). Upon validation against reference data obtained using a mechanical bone contact scanner, MR- and CT-based models were found to contain errors of 0.23±0.20 and 0.07±0.02 mm, respectively.[21,22]

The movement between the neutral and abducted position was interpolated based on the principles put forth by Sahara, et al.,[23] who showed that the movement of joint osseous structures can be defined as a combination of rotational and translational movements about the instantaneous axis of rotation of the joint. In the simulation, we interpolated the motion of the scapula about a screw axis of the shoulder complex, which is similar to the actual motion of the scapula in vivo (Fig. 2B).

Evaluating SSN movement during shoulder abduction

SSN movement was evaluated using finite element modeling and the linear elasticity theory. The SSN was represented as a set of 12320 hexahedral elements, with material properties equivalent to those of rat nerves (Young's modulus, 0.58 MPa; Poisson's ratio, 0.42).[24] The triangular elements making up the surface of the bony structure were converted directly to quadrilateral elements to build a rigid-body mesh. The finite element models of the scapula, clavicle, and spine-rib complex contained 28289, 3863, and 954324 elements, respectively.

The finite element models were analyzed using the Abaqus/Explicit code (Dassault Systèmes, Waltham, MA, USA) to track

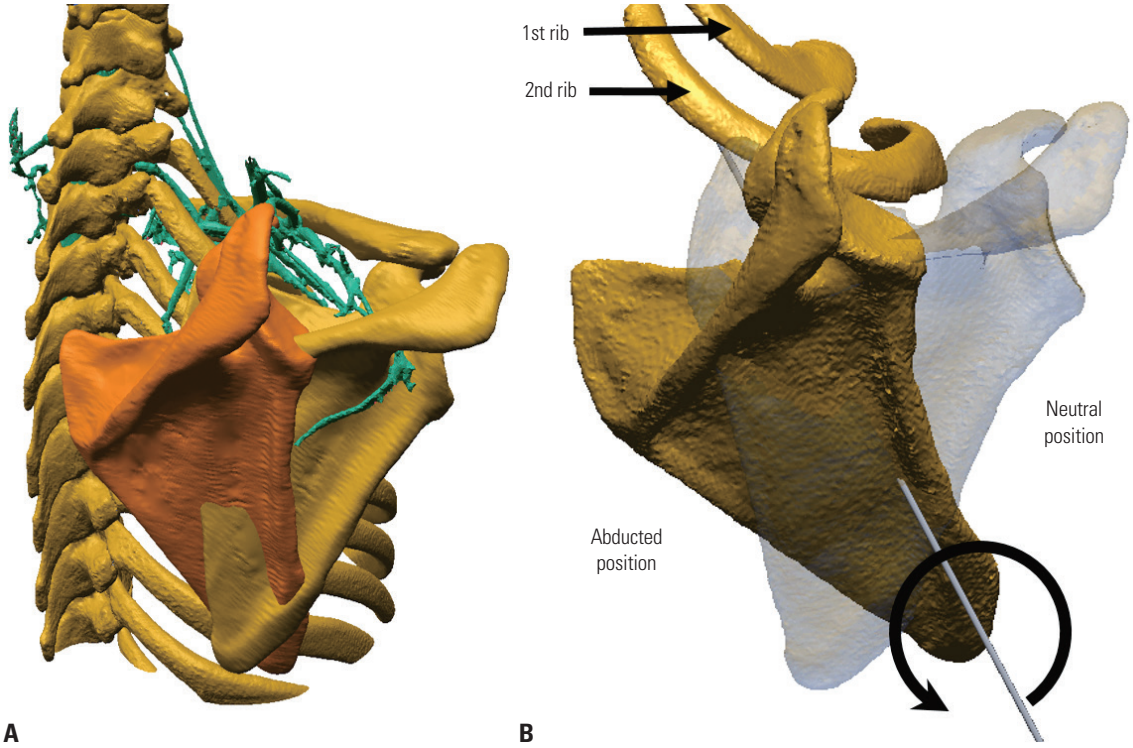

Fig. 2. Simulating shoulder abduction based on two positions of the shoulder complex with the scapula in a neutral or abducted position. (A) The neutral and abducted scapulae were overlapped by matching the respective spine-rib models reconstructed from BP-MR and oblique CT images. (B) Shoulder abduction was simulated as rotation about the instantaneous axis of rotation calculated based on the relative position of the two overlapped scapulae. BP-MR, magnetic resonance imaging of the brachial plexus; CT, computed tomography.

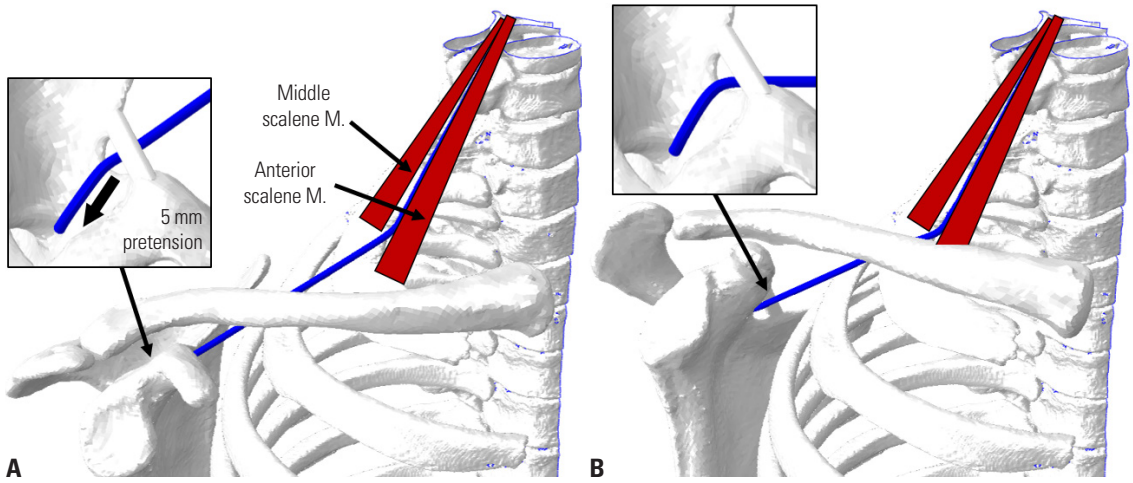

Fig. 3. Application of boundary conditions to the simulation. Any unrealistic motion of the root and trunk during simulated shoulder abduction was minimized by implementing the following boundary conditions: incorporating the clavicle and the anterior and posterior edges of the scalene muscles into the model; applying pretension in the form of 5-mm elongation. (A) Neutral. (B) Abduction.

the change in SSN position as the scapula moved from the neutral to the abducted position. Scapular movement was measured as displacement with respect to the rotational axis. Throughout shoulder abduction, the contact pattern of the SSN according to the axial direction with the TSL or the base of the suprascapular notch was observed. The model and boundary conditions used in the simulation are illustrated in Fig. 3A.

From the simulation, we measured the contact stress on the SSN as the scapula moved sequentially from the neutral to the abducted position (Fig. 3B). Contact stress was measured at the point of maximum contact between the SSN and TSL or suprascapular notch in each position along the transition between neutral and abducted position. The maximal contact stress was measured at a peak point where the contact stress between the SSN and TSL or suprascapular notch was highest.

https://doi.org/10.3349/ymj.2022.63.7.657

RESULTS

In the neutral position, the SSN ran parallel to the front of the TSL until entering the suprascapular notch. From the neutral to the abducted position, the scapula performed upward scapular rotation, posterior tilt, and external rotation of 39.57°, 21.08°, and 14.38°, respectively.

In the neutral position, the SSN contacted the anteroinferior surface of the TSL (Fig. 4A), and the contact stress on the SSN was estimated at 0.06 MPa. Contact stress decreased as the SSN lost contact to the TSL and moved toward the center of the suprascapular notch in the early phase of shoulder abduction (Fig. 4B), but increased again at the end of shoulder abduction (Fig. 4C) as the SSN began to contact the base of the suprascapular notch. The pattern of contact stress according to scapular rotation is illustrated in Fig. 5A.

In the simulation involving a TSL-free scapula, there was no contact stress on the SSN in the neutral position, although contact stress toward the end of shoulder abduction was similar to that noted in the simulation involving the TSL-bound scapula, featuring an increase in contact stress as the SSN began to contact the base of the suprascapular notch. The pattern of contact stress according to the rotation of the TSL-free scapula is illustrated in Fig. 5B.

All result values were set as the average value of two measurers, and all measurements were performed twice at an interval of 2 weeks. The inter- intraobserver agreements for results were quantified using κ-statistics. Statistical interpretation was performed as described by Landis and Koch.[25] Interobserver and intraobserver reliabilities revealed excellent results (kappa statistic=0.853, 0.901).

DISCUSSION

The important finding of this study is that the movement of the SSN is confirmed within the suprascapular notch during shoulder abduction. The findings of our study provide an understanding of the potential mechanisms underlying SSN entrapment, indicating that certain characteristics of scapular position and motion may aggravate or mitigate SSN entrapment. Specifically, we found that, in the neutral position, the SSN contacted the anterior surface of the TSL; as scapular motion, including posterior tilt and upward rotation, progressed towards the abducted position, the SSN moved away from the TSL and shifted toward the base of the suprascapular notch, resulting in secondary contact. The change in the SSN position within the suprascapular notch was due to a change in the entry angle of the SSN. These findings highlight the importance of the spatial relationship between the suprascapular notch and the SSN passing under the TSL.

Our present findings suggest that scapular dyskinesis caused by an anterior tilt of the scapula, thoracic kyphosis, contracture of the pectoralis minor muscle, or dysfunction of the serratus anterior muscle may predict SSN entrapment.[26-28] Specifically, anterior scapular tilt forces the SSN to adopt a more acute entry into the suprascapular notch, increasing the chance that the SSN would contact the TSL at some point during shoulder abduction. Meanwhile, posterior scapular tilt reduces the risk of TSL contact by forcing the SSN to pass vertically through the center of the notch. Thus, even if there is no abnormality in the movement and position of the scapula, the SSN can be entrapped in the neutral position in individuals with a hypertrophied TSL, notch stenosis, or specific anatomy of the vessels around the notch.

In addition, because the simulation involving a TSL-free scapula revealed no contact stress on the SSN in the neutral position, our findings support the validity of TSL release for managing SSN entrapment syndrome. TSL release would thus be effective for both entrapment scenarios: abnormal scapular position and anatomical variations of the TSL.

The first study to describe SSN movement due to scapular motion was conducted by Massimini, et al.[29] According to their cadaveric study, the position of the SSN within the notch during shoulder abduction was affected by TSL release, rotator cuff tear, and repair. Although the shoulder abduction task used in

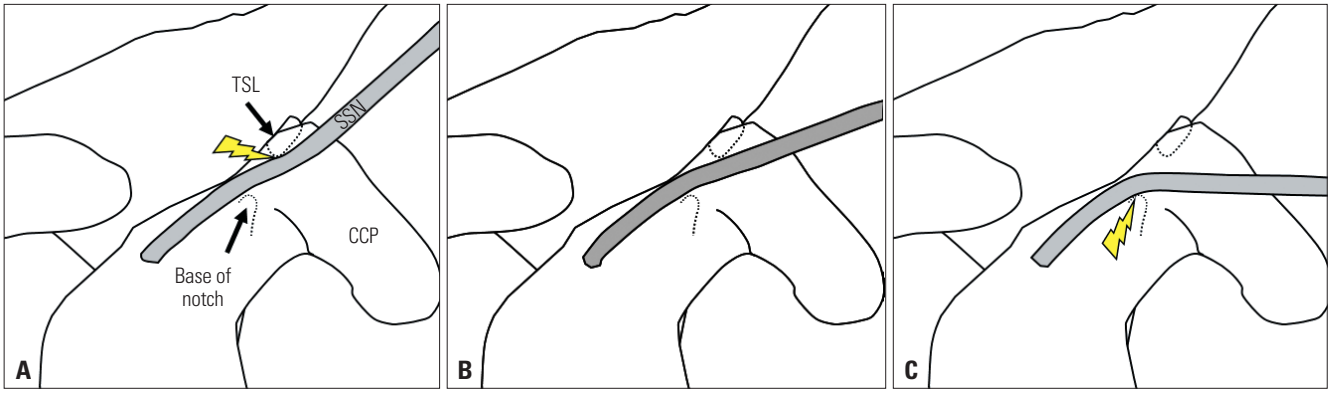

Fig. 4. Schematic diagram of the SSN contact and its surrounding structure during shoulder abduction. (A) Neutral. (B) Mid-abduction. (C) Full abduction. SSN, suprascapular nerve; TSL, transverse scapular ligament; CCP, coracoid process.

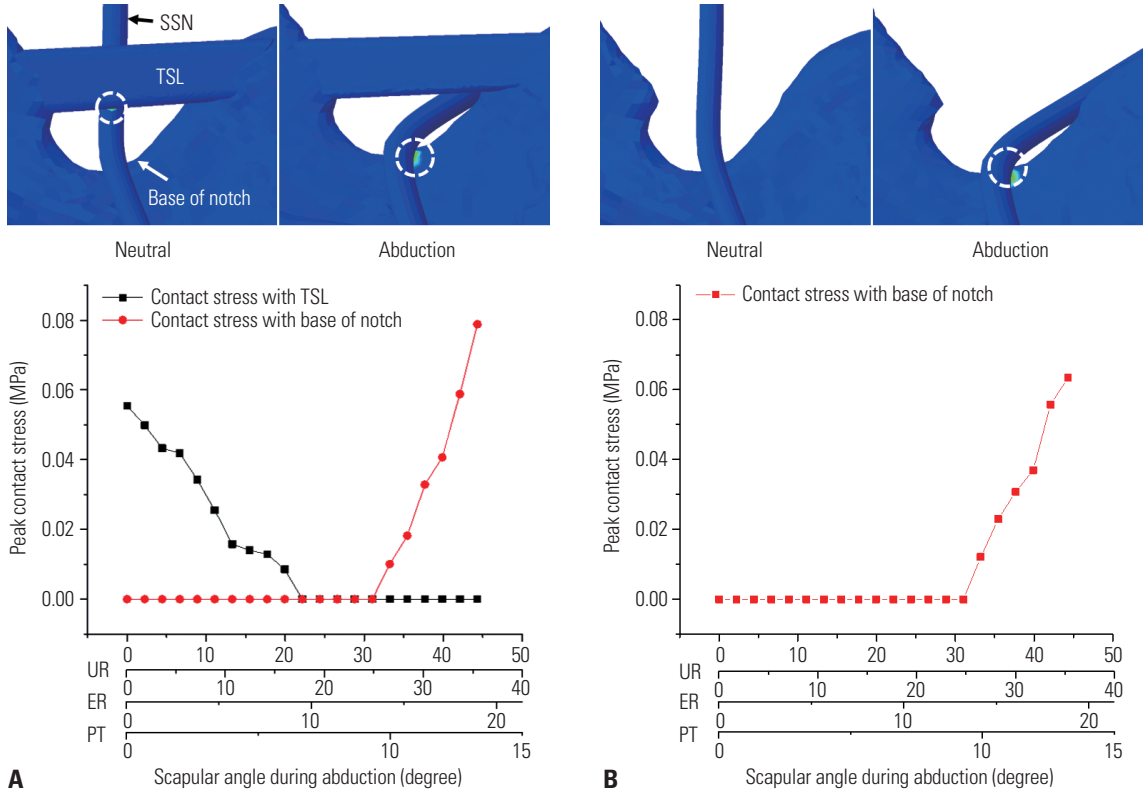

Fig. 5. Change in SSN contact stress according to the shoulder abduction angle. Distribution of contact stress on the SSN in the neutral and abducted positions of the TSL-bound scapula (A) and TSL-free scapula (B). UR, upward rotation; ER, external rotation; PT, posterior tilt; SSN, suprascapular nerve; TSL, transverse scapular ligament.

their study could not reproduce the in vivo movement of the shoulder, their findings drew attention to the possibility of dynamic entrapment of the SSN within the suprascapular notch during scapular movement.

To reproduce the in vivo movement of the scapula, we used an MR image of the shoulder with the scapula in neutral position, as well as a CT image of the shoulder with the scapula in arm abducted position. We superimposed the spine-rib complex in the MR and CT images to obtain overlapped scapulae in different positions, which enabled us to calculate the axis of instantaneous rotation and subsequently simulate continuous scapular movement about this axis. Although it is difficult to quantify the differences between the actual scapular movement in vivo and the simulated shoulder abduction movement based on the two static images used in this study, the differences are expected to be negligible, as reflected in a study of shoulder abduction patterns.[30] However, the method used in this study cannot reproduce movement outside the simulated path between the two states: such movements include instantaneous downward rotation of the scapula in the early stage of humeral elevation, as observed in the normal population, or irregular, uncoordinated movement of the scapula in patients with scapular dyskinesis.[31,32]

In order to accurately reproduce shoulder abduction, it is necessary to account for morphological discrepancies in abduction-neutral positions. In the present study, we attempted to minimize such morphological discrepancies by carefully recording the positions of the first and second ribs and cervical/upper thoracic vertebrae, which are considered the least affected by spatial alterations of the ribs and spine due to breathing and humeral abduction. Errors may also be introduced when reconstructing 3D images based on data from different sources. However, a previous study reported that CT- and MR-based models did not differ substantially (0.23±0.20 mm).[33]

Van de Velde, et al.[34] obtained MR-based 3D models of the BP and SSN branching from the upper trunk, reporting that such models reconstructed based on in vivo MR images are equivalent to those obtained based on anatomic dissection. Although in vivo 3D reconstruction has limitations that cannot be overcome, 3D reconstructed models can be safely compared if they do not deviate from the contour of the actual BP or if their deviation is similar. In the present study, the 3D BP-SSN models reconstructed from in vivo MR and CT images, in which the contours were drawn by independent observers according to the same procedure described above, revealed the same course and branching patterns, suggesting high inter-observer reliability.

There are several limitations to the present study. One of the limitations was that the simulation protocol applied in this study has innate limitations. As a result, we cannot rule out

https://doi.org/10.3349/ymj.2022.63.7.657

various processing errors that may affect the results. The second limitation in this study is that we used data from only one patient, because only one of eight candidates obtained fine modeling. As a result, individual differences in scapular movement could not be explained. However, the shoulder abduction motion simulated in this study clearly reflected various types of upward/downward, anterior/posterior, and internal/external rotation. Thus, from a biomechanical perspective, the pattern of dynamic SSN entrapment during scapular movement can be accurately predicted independently of the individual differences. Specifically, the results of our investigation suggest that risk factors for static or dynamic SSN entrapment include any scapular movement inducing anterior tilt, TSL thickening, and a shallow suprascapular notch. Further research may be needed through more modeling in the near future. Finally, although the clinical results were good in all patients who performed TSL release, there was a clinical limitation in that the results did not go through a detailed outcome analysis process, and a comparative analysis through the control group was not performed.

We identified changes in the position of the SSN path within the suprascapular notch during shoulder abduction. The SSN starts in contact with the TSL and moves toward the base of the suprascapular notch, with secondary contact. Accordingly, these results suggest that TSL release may be a feasible treatment option for dynamic SSN entrapment.

ACKNOWLEDGEMENTS

This research was supported by Basic Science Research Program through the National Research Foundation of Korea (NRF) funded by the Ministry of Education (NRF-2016R1D1A1A09920056).

AUTHOR CONTRIBUTIONS

Conceptualization: Yon-Sik Yoo. Data curation: Jung-Ah Choi and Jung Hyun Oh. Formal analysis: Yon-Sik Yoo and Jeung Yeol Jeong. Funding acquisition: Yon-Sik Yoo. Investigation: Jung-Ah Choi. Methodology: Seong-wook Jang and Yoon Sang Kim. Project administration: Jeung Yeol Jeong. Resources: Jung Hyun Oh. Software: Seong-wook Jang. Supervision: Jeung Yeol Jeong. Validation: Yon-Sik Yoo and Jeung Yeol Jeong. Writing—original draft: Yon-Sik Yoo and Seong-wook Jang. Writing—review & editing: Jeung Yeol Jeong. Approval of final manuscript: all authors.

ORCID iDs

Yon-Sik Yoo https://orcid.org/0000-0002-2497-7786
Seong-wook Jang https://orcid.org/0000-0003-4696-2291
Yoon Sang Kim https://orcid.org/0000-0002-0416-7938
Jung-Ah Choi https://orcid.org/0000-0002-0896-4766
Jung Hyun Oh https://orcid.org/0000-0003-3217-389X
Jeung Yeol Jeong https://orcid.org/0000-0001-8145-1302

REFERENCES

1. Budzik JF, Wavreille G, Pansini V, Moraux A, Demondion X, Cotten A. Entrapment neuropathies of the shoulder. Magn Reson Imaging Clin N Am 2012;20:373-91, xii.
2. Barber FA. Percutaneous arthroscopic release of the suprascapular nerve. Arthroscopy 2008;24:236.e1-4.
3. Barwood SA, Burkhart SS, Lo IK. Arthroscopic suprascapular nerve release at the suprascapular notch in a cadaveric model: an anatomic approach. Arthroscopy 2007;23:221-5.
4. Bhatia DN, de Beer JF, van Rooyen KS, du Toit DF. Arthroscopic suprascapular nerve decompression at the suprascapular notch. Arthroscopy 2006;22:1009-13.
5. Ghodadra N, Nho SJ, Verma NN, Reiff S, Piasecki DP, Provencher MT, et al. Arthroscopic decompression of the suprascapular nerve at the spinoglenoid notch and suprascapular notch through the subacromial space. Arthroscopy 2009;25:439-45.
6. Kim SH, Kim SJ, Sung CH, Koh YG, Kim YC, Park YS. Arthroscopic suprascapular nerve decompression at the suprascapular notch. Knee Surg Sports Traumatol Arthrosc 2009;17:1504-7.
7. Cummins CA, Messer TM, Nuber GW. Suprascapular nerve entrapment. J Bone Joint Surg Am 2000;82:415-24.
8. Plancher KD, Luke TA, Peterson RK, Yacoubian SV. Posterior shoulder pain: a dynamic study of the spinoglenoid ligament and treatment with arthroscopic release of the scapular tunnel. Arthroscopy 2007;23:991-8.
9. Post M, Mayer J. Suprascapular nerve entrapment. Diagnosis and treatment. Clin Orthop Relat Res 1987;223:126-36.
10. Rengachary SS, Neff JP, Singer PA, Brackett CE. Suprascapular entrapment neuropathy: a clinical, anatomical, and comparative study. Part 1: clinical study. Neurosurgery 1979;5:441-6.
11. Romeo AA, Ghodadra NS, Salata MJ, Provencher MT. Arthroscopic suprascapular nerve decompression: indications and surgical technique. J Shoulder Elbow Surg 2010;19(2 Suppl):118-23.
12. Tasaki A, Nimura A, Mochizuki T, Yamaguchi K, Kato R, Sugaya H, et al. Anatomic observation of the running space of the suprascapular nerve at the suprascapular notch in the same direction as the nerve. Knee Surg Sports Traumatol Arthrosc 2015;23:2667-73.
13. Shimoe T, Doi K, Madura T, Kumar KK, Montales TD, Hattori Y, et al. Analysis of shoulder abduction by dynamic shoulder radiograph following suprascapular nerve repair in brachial plexus injury. J Orthop Sci 2017;22:840-5.
14. Daripelli S, Tolupunoori B, Vinodini L. Morphometric study of suprascapular notch and its safe zone in Indian population. Maedica (Bucur) 2020;15:461-7.
15. Dixon WT. Simple proton spectroscopic imaging. Radiology 1984;153:189-94.
16. Lorensen WE, Cline HE. Marching cubes: a high resolution 3D surface construction algorithm. ACM Siggraph Computer Graphics 1987;21:163-9.
17. Polguj M, Rożniecki J, Sibiński M, Grzegorzewski A, Majos A, Topol M. The variable morphology of suprascapular nerve and vessels at suprascapular notch: a proposal for classification and its potential clinical implications. Knee Surg Sports Traumatol Arthrosc 2015;23:1542-8.
18. Polguj M, Sibiński M, Grzegorzewski A, Waszczykowski M, Majos A, Topol M. Morphological and radiological study of ossified superior transverse scapular ligament as potential risk factor of suprascapular nerve entrapment. Biomed Res Int 2014;2014:613601.
19. Kibler WB, Ludewig PM, McClure PW, Michener LA, Bak K, Sciascia AD. Clinical implications of scapular dyskinesis in shoulder injury: the 2013 consensus statement from the 'Scapular Summit.' Br

J Sports Med 2013;47:877-85.
20. Wu G, van der Helm FC, Veeger HE, Makhsous M, Van Roy P, Anglin C, et al. ISB recommendation on definitions of joint coordinate systems of various joints for the reporting of human joint motion--Part II: shoulder, elbow, wrist and hand. J Biomech 2005;38:981-92.
21. Jang SW, Ko J, Yoo YS, Kim Y. An evaluation on CT image acquisition method for medical VR applications. Proceedings of the Eighth International Conference on Graphic and Image Processing (ICGIP 2016); 2016 Oct 29-31; Tokyo, Japan: SPIE; 2017. p.102250S.
22. Rathnayaka K, Momot KI, Noser H, Volp A, Schuetz MA, Sahama T, et al. Quantification of the accuracy of MRI generated 3D models of long bones compared to CT generated 3D models. Med Eng Phys 2012;34:357-63.
23. Sahara W, Sugamoto K, Murai M, Tanaka H, Yoshikawa H. 3D kinematic analysis of the acromioclavicular joint during arm abduction using vertically open MRI. J Orthop Res 2006;24:1823-31.
24. Borschel GH, Kia KF, Kuzon WM Jr, Dennis RG. Mechanical properties of acellular peripheral nerve. J Surg Res 2003;114:133-9.
25. Landis JR, Koch GG. The measurement of observer agreement for categorical data. Biometrics 1977;33:159-74.
26. Seitz AL, McClure PW, Lynch SS, Ketchum JM, Michener LA. Effects of scapular dyskinesis and scapular assistance test on subacromial space during static arm elevation. J Shoulder Elbow Surg 2012;21:631-40.
27. Bullock GS, Strahm J, Hulburt TC, Beck EC, Waterman BR, Nicholson KF. Relationship between clinical scapular assessment and scapula resting position, shoulder strength, and baseball pitching kinematics and kinetics. Orthop J Sports Med 2021;9:232596712 1991146.
28. Burkhart SS, Morgan CD, Kibler WB. The disabled throwing shoulder: spectrum of pathology part I: pathoanatomy and biomechanics. Arthroscopy 2003;19:404-20.
29. Massimini DF, Singh A, Wells JH, Li G, Warner JJ. Suprascapular nerve anatomy during shoulder motion: a cadaveric proof of concept study with implications for neurogenic shoulder pain. J Shoulder Elbow Surg 2013;22:463-70.
30. Takagi Y, Oi T, Tanaka H, Inui H, Fujioka H, Tanaka J, et al. Increased horizontal shoulder abduction is associated with an increase in shoulder joint load in baseball pitching. J Shoulder Elbow Surg 2014;23:1757-62.
31. Borsa PA, Timmons MK, Sauers EL. Scapular-positioning patterns during humeral elevation in unimpaired shoulders. J Athl Train 2003;38:12-7.
32. Roche SJ, Funk L, Sciascia A, Kibler WB. Scapular dyskinesis: the surgeon's perspective. Shoulder Elbow 2015;7:289-97.
33. Shah AA, Butler RB, Sung SY, Wells JH, Higgins LD, Warner JJ. Clinical outcomes of suprascapular nerve decompression. J Shoulder Elbow Surg 2011;20:975-82.
34. Van de Velde J, Audenaert E, Speleers B, Vercauteren T, Mulliez T, Vandemaele P, et al. An anatomically validated brachial plexus contouring method for intensity modulated radiation therapy planning. Int J Radiat Oncol Biol Phys 2013;87:802-8.

https://doi.org/10.3349/ymj.2022.63.7.657